

Brushless DC motor speed regulation with a fuzzy PID controller

M.GIRIBABU¹,Y.DAVIDU²,
ASSOCIATE PROFESSOR¹, ASSISTANT PROFESSOR²,
DEPARTMENT OF EEE

PBR VISVODAYA INSTITUTE OF TECHNOLOGY AND SCIENCE::KAVALI

Abstract

This paper introduces a unique hybrid control method for speed management of a Brushless DC (BLDC) motor, in which the reference current of the BLDC motor and the voltage on the DC bus of the converter are both controlled at the same time. The DC bus voltage of the converter is controlled by a fuzzy logic controller, and the reference current of the BLDC motor is regulated by a fractional-order proportional-integral-derivative (FOPID) controller. To optimize the FOPID controller's settings, we create a meta-heuristic approach based on a tweaked version of the harmony search (HS) algorithm. The motor is put through a battery of tests under no-load, variable-load, and variable-speed circumstances to ensure the suggested driver works as intended. The suggested mixed control strategy has also been compared to speed control strategies based on Fuzzy logic and FOPID. The findings acquired verify that the suggested control system offers superior and precise speed regulation over a broad speed range. Furthermore, the suggested controller lessens torque waves in a variety of operational contexts.

1 Introduction

Traditional DC motors have many advantages, including simple operation, high efficiency, and favorable speed-to-torque properties. A mechanical commutator, however, and brushes lead to igniting problems and frequent upkeep because of brush wear and strain [1]. To overcome these shortcomings, the brushless DC (BLDC) motor has been created. As a result, BLDC motors have additional benefits, including a wider speed range, quicker rapid reaction, less upkeep, a longer life span, and noiseless operation. Since the BLDC motor packs more power into a smaller package than its competitors, it excels in situations where room is at a premium. These benefits have led to a rise in demand for BLDC motors in many different fields, such as automobiles, aircraft, robotics, and industrial automation [2, 3, and 4]. Some examples of where this is used are in

electric and hybrid cars, compressors, pumps, fans, dryers, medical equipment, motors, CNC machines, and computer hard drives [1]. The three-phase BLDC motor is the most common form of this rotating Synchronous motor with a triangular back-EMF configuration. Permanent magnet rotor made of ferrite magnets or rare earth metal magnets [1] and three-phase co centered windings on the stator. Commutation uses a solid-state electrical controller to electricity electrical inverter or other mechanical component rotational location, which can be determined indirectly by measuring hall-effect sensor or approximated from external sources indications for engine power or amperage [2]. In spite of the quickened as advancement in the field of control theory, the proportionate still widely used today is the integral derivative (PID) controller in the business world because of its simple layout and multiple methods of adjusting being easily accessible. As of late, fractional- academics and control engineers have paid a lot of attention to first-order computers (FOC) because of their adaptability. That these devices have [3, 4]. The Flags of Convenience use a form of calculus known as fractional calculus to non-integer-order differential differentiation and integration ad_ function boundaries of action are outlined in by _ and t, where _ R [5] is the standard sequence of operations. Different fractional-order processors have been proposed in the books. Been developed, including TID (Tilted-integral-derivative). Partial lead-lag correction and (Companies de Renseignements DONE (Crone of the Non-Entering) [6, 7]. The most typical dividing by fraction device is the PID controller with a partial (FOPID) driver, which Podlubny introduced in [8]. The Non-integer-order derivatives were first implemented in the FOPID controller. S_ and s_, a sum of non-integer value. Because of this, more design flexibility despite an increase in factors than the standard PID Controller [9]. Tuning for FOPID is more difficult than conventional there are five adjustable settings for the PID processor. FOPID controller tuning strategies as described in [10]. Could be broken down into one of three types: rule-based techniques, techniques based on analysis and computation. Classes II and III optimization techniques, as well as evolving programs, which excel in their capacity for a worldwide search [11]. There have been many

different evolving methods used. Evolutionary algorithms [12] and other methods for FOPID adjusting gravity probe, firefly experiment, and particle swarm [15]. In contrast, flexible logic management is frequently used in Fuzzy set theory is brilliantly applied here, enabling incomplete affiliations as opposed to the clean set theory.

The flexible logic controller (FLC) does not require a formal model of the regulated system in order to function. Like a chart, it information about the plant's input vectors into a numerical output using language phrases in the form of If-Then patterns [16]. For the purpose of controlling the speed of BLDC motors, both model reference adaptive control (MRAC) and auto-tuning fuzzy PID control were devised in [17], with MRAC demonstrating superior performance. The linear zed model used to describe the BLDC motor is valid only in the neighborhood of the linearization zone. Since the MRAC was developed using a linear model, its efficacy as a driver may suffer outside of the linearization area. Therefore, improving system performance and accommodating for changes in working circumstances can be achieved by incorporating fuzzy logic into the management of the converter DC bus voltage. This paper proposes a method for controlling the speed of BLDC motors using a fuzzy logic controller for the DC inverter voltage and a FOPID controller for the reference current flowing into the BLDC motor from the inverter gate circuit. Both processors will operate in tandem to smooth out torque fluctuations and minimize the amount by which the recorded speed varies from the reference speed. The remaining sections of the text are structured as follows. Section 2 describes the conceptual paradigm, and Section 3 explains how BLDC motor drives work in practice. In Section 4, we see examples of the Fuzzy and FOPID controller designs. The FOPID adjustment using the harmony search algorithm is presented in Section 5, while modeling findings and comments are given in Section 4.

2 The Mathematical Modeling

The corresponding circuit for a BLDC motor transmission is depicted in Fig. 1. The formulae for the phase values of the armature windings as

$$V_a = R_a i_a + \frac{d}{dt} (L_{aa} i_a + L_{ba} i_b + L_{ca} i_c) + E_a \quad (1)$$

$$V_b = R_b i_b + \frac{d}{dt} (L_{bb} i_b + L_{ab} i_a + L_{cb} i_c) + E_b \quad (2)$$

$$V_c = R_c i_c + \frac{d}{dt} (L_{cc} i_c + L_{bc} i_b + L_{ac} i_a) + E_c \quad (3)$$

Where a, b, and c are currents through the armature and Ra, Rb, and Rc are resistances through the armature. EMFs Ea, Eb, and Ec have returned. Mutual inductances include Lab, Lba, Lac, Lca, Lcb, and Lcc, while self-inductances include Laa, Lbb, and Lcc. If we assume that Ra = Rb = and that the rotor reluctances are constant regardless of the rotational inclination, we get:

$$L_{aa} = L_{bb} = L_{cc} = L \quad (4)$$

$$L_{ab} = L_{ba} = L_{ac} = L_{ca} = L_{ca} = L_{bc} = M \quad (5)$$

The grid representation of the BLDC motor model looks like this:

$$\begin{bmatrix} V_a \\ V_b \\ V_c \end{bmatrix} = \begin{bmatrix} R & 0 & 0 \\ 0 & R & 0 \\ 0 & 0 & R \end{bmatrix} + \begin{bmatrix} L & M & M \\ M & L & M \\ M & M & L \end{bmatrix} \left(\frac{d}{dt} \right) \begin{bmatrix} i_a \\ i_b \\ i_c \end{bmatrix} + \begin{bmatrix} E_a \\ E_b \\ E_c \end{bmatrix} \quad (6)$$

However, according to Kirchhoff's current law

$$i_a + i_b + i_c = 0$$

Therefore,

$$M i_b + M i_c = -M i_a \quad (8)$$

Then

$$\begin{bmatrix} V_a \\ V_b \\ V_c \end{bmatrix} = \begin{bmatrix} R & 0 & 0 \\ 0 & R & 0 \\ 0 & 0 & R \end{bmatrix} + \begin{bmatrix} L-M & 0 & 0 \\ 0 & L-M & 0 \\ 0 & 0 & L-M \end{bmatrix} \left(\frac{d}{dt} \right) \begin{bmatrix} i_a \\ i_b \\ i_c \end{bmatrix} + \begin{bmatrix} E_a \\ E_b \\ E_c \end{bmatrix} \quad (9)$$

The induced back-EMFs are

$$E_a = f_a(\theta_r) * \beta_p * \omega \tag{10}$$

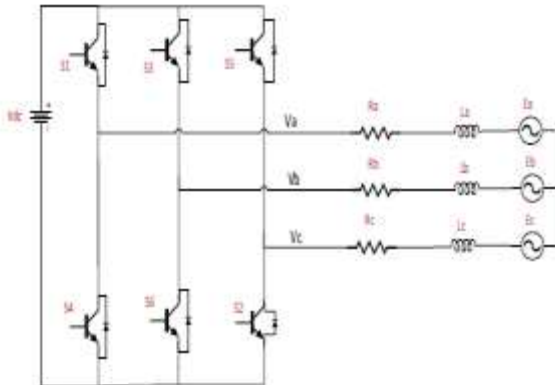
$$E_b = f_b(\theta_r) * \beta_p * \omega \tag{11}$$

$$E_c = f_c(\theta_r) * \beta_p * \omega \tag{12}$$

$$f_a(\theta_r) = \begin{cases} 1, & 0 \leq \theta_r \leq \frac{2\pi}{3} \\ 1 - \frac{6}{\pi} \left(\theta_r - \frac{2\pi}{3} \right), & \frac{2\pi}{3} \leq \theta_r \leq \pi \\ -1, & \pi \leq \theta_r \leq \frac{5\pi}{3} \\ -1 + \frac{6}{\pi} \left(\theta_r - \frac{5\pi}{3} \right), & \frac{5\pi}{3} \leq \theta_r \leq 2\pi \end{cases} \tag{13}$$

The functions $f_b(\theta_r)$ and $f_c(\theta_r)$ are given as

$$\begin{aligned} f_b(\theta_r) &= f_a\left(\theta_r - \frac{2\pi}{3}\right) \\ f_c(\theta_r) &= f_a\left(\theta_r - \frac{4\pi}{3}\right) \end{aligned} \tag{14}$$



BLDC motor equivalent circuit shown in Fig. 1.

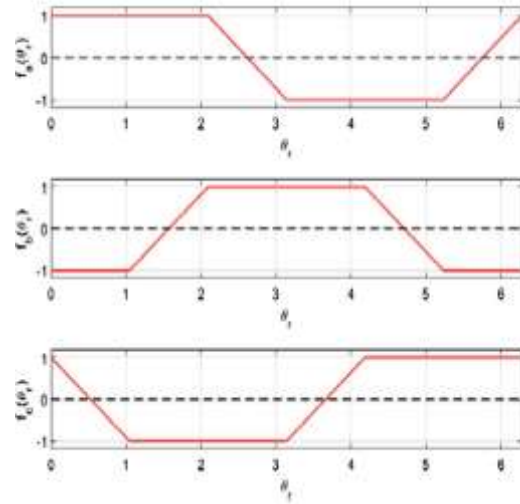


Table 1 BLDC motor parameters

Parameter	Value
Voltage	48 V
Poles	4
Torque constant	0.14 N.m/A
Voltage constant	10.4 V/KRPM
Rated torque	7 N.m
Stator resistance	0.1 O
Stator inductance	10 mH
Rotor inertia	$5 * 10^{-4} kg.m^2$
Rotor friction	$0.001 \frac{N.m}{rad/s}$

When losses due to friction and other sources are disregarded, the formula for electromagnetic torque is:

$$T_e = \frac{E_a i_a + E_b i_b + E_c i_c}{\omega} \tag{15}$$

The load torque and electromagnetic torque are related by:

$$T_e - T_l = J \frac{d\omega}{dt} + B_v \omega \tag{16}$$

$$T_e - T_l = J \frac{d\omega}{dt} + B_v \omega \tag{16}$$

Where T_l represents the load force, J represents the moment of inertia of the rotor, and B represents the viscous friction rate. The aforementioned BLDC

motor model formulae can be state-space-representation-wise, they are

$$\frac{d}{dt} \begin{bmatrix} i_a \\ i_b \\ i_c \\ \omega \end{bmatrix} = \begin{bmatrix} -\frac{R}{L} & 0 & 0 & 0 \\ 0 & -\frac{R}{L} & 0 & 0 \\ 0 & 0 & -\frac{R}{L} & 0 \\ \frac{K_t}{J} & \frac{K_t}{J} & \frac{K_t}{J} & -\frac{1}{J} \end{bmatrix} \begin{bmatrix} i_a \\ i_b \\ i_c \\ \omega \end{bmatrix} + \begin{bmatrix} \frac{1}{L} & 0 & 0 & 0 \\ 0 & \frac{1}{L} & 0 & 0 \\ 0 & 0 & \frac{1}{L} & 0 \\ 0 & 0 & 0 & -\frac{1}{J} \end{bmatrix} \begin{bmatrix} V_a \\ V_b \\ V_c \\ T \end{bmatrix} \quad (17)$$

Table 2 Gate switching signals

Rotor angle (rad)	Closed switches	Phase current		
		A	B	C
$0 - \pi/3$	S6 S1	+	-	OFF
$\pi/3 - 2\pi/3$	S2 S1	+	OFF	-
$2\pi/3 - \pi$	S2 S3	OFF	+	-
$\pi - 4\pi/3$	S4 S3	-	+	OFF
$4\pi/3 - 5\pi/6$	S4 S5	-	OFF	+
$5\pi/6 - 2\pi$	S6 S5	OFF	-	+

Where $L_s = M - L$. Motor parameters are shown in Table 1

3 Drive Operation Principles

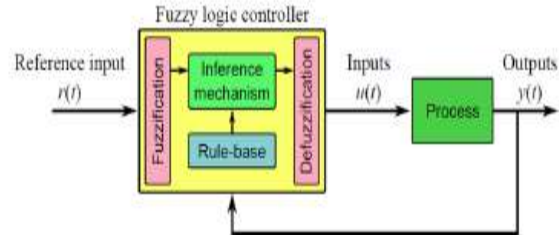
The BLDC motor drive shown in Fig. 1 operates by alternately activating the motor's two stages based on the rotor position data. Three hall-effect sensors, spaced 120 degrees apart, detect the north and south poles of the rotor and send a 1 or 0 indication, accordingly. The state of MOSFET switches S1–S6 is controlled by gate impulses based on readings from hall-effect sensors. The gate switching indications and phase current state per rotor location are shown in Table 2 below.

4 Speed Controller Design

Fuzzy Controller

In Fig. 3, we see the usual components that make up a fuzzy control system, which are as follows: (1) Fuzzification, which translates the incoming numbers into a metaphor. (2) A database containing IF-THEN algorithms. (3) Inference mechanism, which infers language factors and control principles to produce imprecise control action. (4) Defuzzification, which

converts the result of the reasoning method into a number for use as a regulating parameter [16]. The magnitude of the DC bus voltage in the converter is what the suggested fuzzy controller is meant to regulate. The intended motor speed and the rate of change in the mistake between these two speeds serve as the controller's inputs, respectively.



The DC bus voltage shown as the standard number in Fig. 3 is the controller's output in a fuzzy logic control system. Membership algorithms based on triangles are used. Accommodating ambiguous sources and outputs. With a unified input range of -3 to 3, the input universe of discourse is represented by [Extra Small(ES), Very Small(VS), Small(S), Medium(M), Large(L), Very Large(VL), Extra Large(EL)], and the output universe of discourse is represented by [Extra Large(EL), Very Large(VL), Extra Large(EL)], with a range of 0 to 50. The principles used to create the fuzzy controller are shown in Table 3, and the membership functions used for the inputs and outputs are shown in Figure 4.

4.2 Fractional Order PID (FOPID) Controller

Differential equation representation of FOPID is given as:

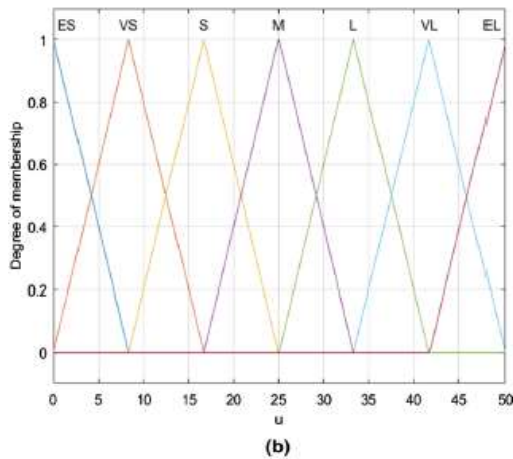
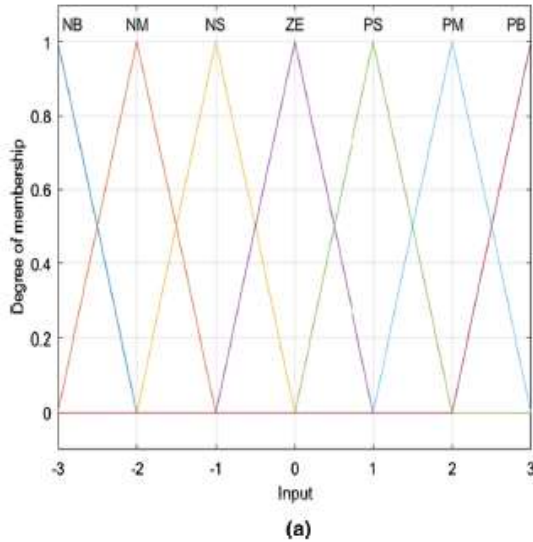
$$u(t) = K_p e(t) + K_i D_t^{-\lambda} e(t) + K_d D_t^{\mu} e(t) \quad (18)$$

$$G(s) = K_p + K_i s^{-\lambda} + K_d s^{\mu} \quad (19)$$

where

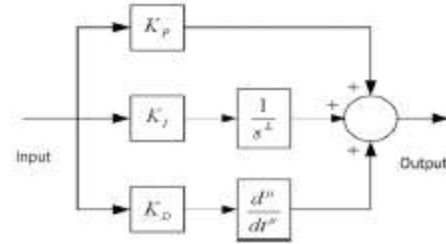
K_p : is proportional constant	K_i : is integral constant
K_d : is derivative constant	λ : is the integration order
μ : is the differentiation order	

The block layout of the Laplace transform-informed FOPID controller is shown in Figure 5.



Membership functions at the inputs (a) and the outputs (b) are shown in Figure 4.

Output variables u	Change in error e							
	NB	NM	NS	Z	PS	PM	PB	
Error e	NB	ES	ES	ES	VS	S	S	M
	NM	ES	ES	VS	S	S	S	S
	NS	VS	S	S	S	M	L	L
	Z	VS	S	S	M	L	L	VL
	PS	S	S	M	L	L	VL	VL
	PM	M	M	L	L	VL	VL	EL
	PB	L	L	VL	VL	EL	EL	EL



Block schematic of a FOPID actuator the purpose of the FOPID driver is to regulate the rotational speed of BLDC motors by modifying the three-phase reference voltage. Hysteresis current driver currents. After that, bursts of inverter gate current are produced to power the motor. In this work, the optimum numbers for the FOPID controller settings are found using the harmony search optimization method.

5 Harmony Search Algorithms

Gem [25] proposed the population-based, musically-inspired Harmony Search Algorithm (HSA). HSA models how musicians improvise, symbolizing the process of experimenting with various tone combos to discover a pleasing balance. This is done in HSA during the choosing procedure by allowing the user to pick the values of the New Harmony from the solution set stored in the Harmony Memory (HM). They can also be picked at random from the allowable range of numbers [26, 27], or selected from HM with a minor tweak. There are two main controls on this process: The rate at which the answer derived from HM is adjusted by a small amount is represented by the pitch-adjusting rate (PAR): PAR [0, 1].

$$x_{new} = x_{old} + FW.r \tag{20}$$

The second is the Harmony Memory Considering Rate (HMCR) [0, 1], which indicates the likelihood of picking a potential answer from among the current participants in the Harmony Memory. HM. Selecting only a limited number of top harmonics at low HMCR values can delay convergence. While resolution is quicker at large values (near 1.0), this may be at the expense of the algorithm's capacity to explore new solutions. Here is a rundown of the steps involved in an HS process [27, 28]: a) randomly produced starting answers in the Harmony Memory (HM). You can write down an HM of dimension HMS like this:

$$HM = \begin{bmatrix} x_1^1 & x_2^1 & \dots & x_n^1 \\ x_1^2 & x_2^2 & \dots & x_n^2 \\ \vdots & \vdots & \dots & \vdots \\ x_1^{HMS} & x_2^{HMS} & \dots & x_n^{HMS} \end{bmatrix} \quad (21)$$

where $[x_1^i, x_2^i, \dots, x_n^i]$ is the candidate solutions, $i=1, 2, \dots, HMS$.

HMCR and PAR are analogous to the genetic algorithms crossing and mutation likelihood and are used in creating New Harmony from the HM. (GA). © HM Updates. Step by's new harmony is judged against the HM's worst harmony. If the New Harmony is more suitable, it will supplant the least desirable one in HM; otherwise, the least desirable one will be removed. If the end condition is not met, the process will loop back to stage (d). The method used is a derivative of the original HS algorithm. However, in order to increase convergence speed, it was suggested that numerous harmonics be generated at once rather than just one. In [29], this adjustment is first mentioned. The following equation [30] has also been used to implement a dynamic FW.

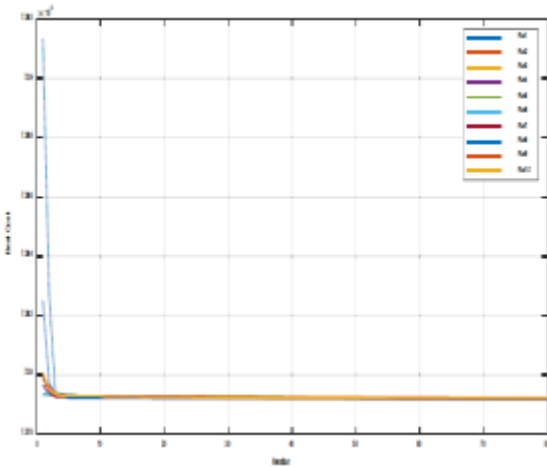


Fig. 6 Solution convergence

$$FW(i) = FW_{\max} \exp \left(\ln \left(\frac{FW_{\min}}{FW_{\max}} \right) * \frac{i}{NI} \right) \quad (22)$$

Where Wax is the largest fret width allowed, FWmin is the smallest fret width allowed, NI is the total number of generations, and I is the generation number currently in effect. Using a Dynamic FW

Method provides an initial large value to improve worldwide search capability, and then progressively declines with increasing rounds so that FW ultimately uses a small value to boost local search performance. By reducing the cost function described by Integral of Square Error (ISE), the following equation is used by HSA to adjust the FOPID constants Kip, Ki, Kd, λ, and μ.

$$ISE = \frac{1}{10000} \int \epsilon^2 dt \quad (23)$$

Where time, t is measured and the motion deviation, ε, is indicated. Here is how we define the inequalities:

$$0.1 \leq K_p \leq 50 \quad (24)$$

$$0.1 \leq K_i \leq 50 \quad (25)$$

$$0.1 \leq K_d \leq 4 \quad (26)$$

$$0.1 \leq \lambda \leq 2 \quad (27)$$

$$0.1 \leq \mu \leq 2 \quad (28)$$

Table 4 Statistics for 10 runs

	Minimum	Maximum	Average
HSA Objective function	73792.19	73792.35	73792.23

Table 5 FOPID controller tuned parameters

Parameter	K_p	K_i	K_d	λ	μ
value	21.88	27.4575	0.8709	1.2189	0.1186

While Table 5 lists the ideal values for all the variables. The suggested optimization method is shown to be stable and to converge to the same value for the goal function. In addition, the answer convergence of the updated harmony search method is shown in Fig. 7 in comparison to particle swarm optimization (PSO). The HSA solution clearly outperforms the PSO solution in terms of the lowest value of the goal function. The objective function assessment in this article's intended system can be

completed in 1.557 s using HSA, while the same task using PSO would take 2.142 s.

6 Simulation Results and Discussions

Both the DC bus voltage and the reference current of the inverter gate circuit are shown in Fig. 8 of the schematic for the suggested hybrid-Fuzzy-FOPID managed systems. Managed concurrently. Three situations were examined to verify the efficiency of the proposed management method. Firstly,

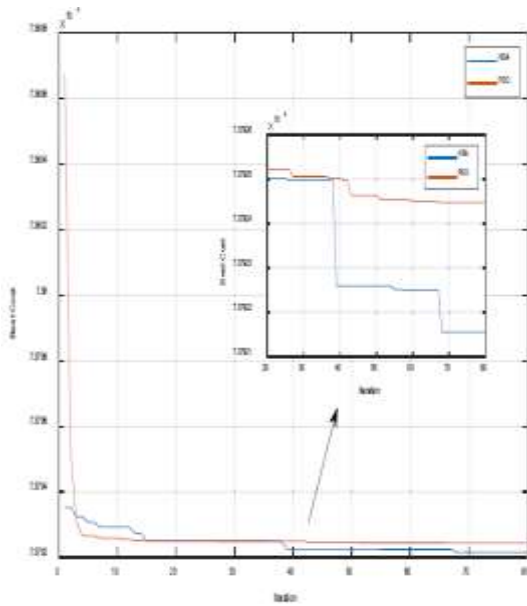
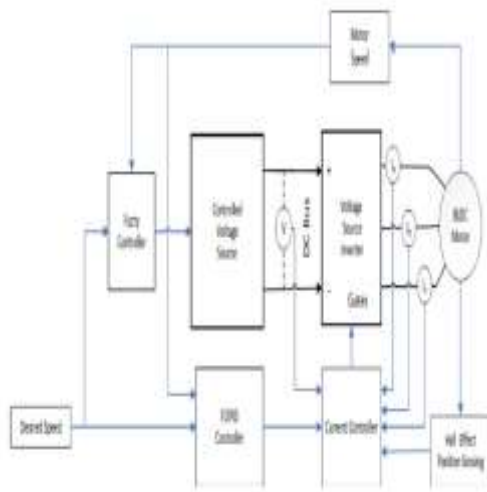


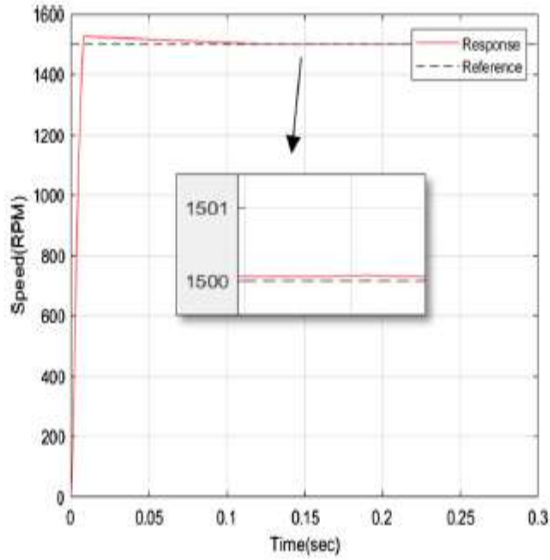
Fig. 7 Solution convergence for HSA and PSO



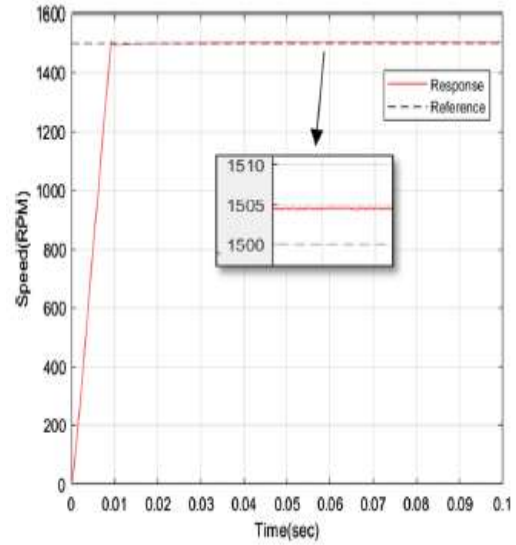
In Fig. 8, the suggested hybrid fuzzy-FOPID speed controller is shown in action during a simulation in which the system is running at a steady pace without any burden. While shifting the pace around. Finally, the weight on the engine has been altered in a sequence while the pace has been held steady. The system has been simulated using MATLAB 2019b. Fuzzy and FOPID-based speed control methods have also been compared to the outcomes for each situation. In order to manage the rotational speed of a brushless DC motor, a fuzzy controller modulates the DC bus voltage, while hall-effect sensors provide information on the rotor's location, which is used to create gate signals for the inverter. The FOPID control system maintains a fixed DC bus voltage while allowing for precise speed regulation via inverter gate current for BLDC motors.

No Load Operation

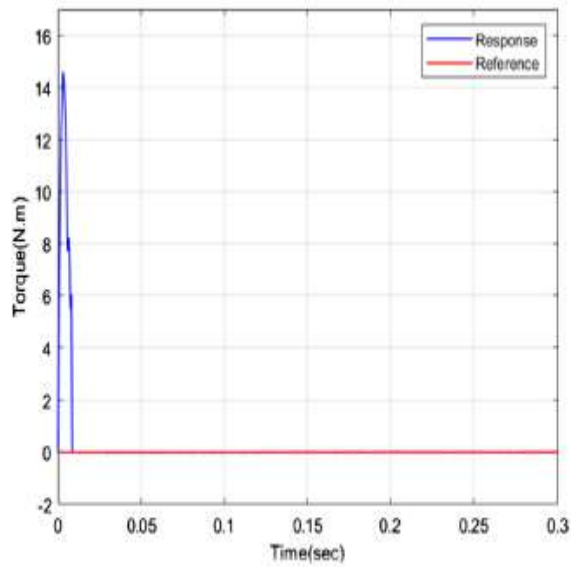
Figures 9, 10, and 11 depict the speed and torque reactions using the fuzzy controller, the FOPID controller, and the suggested hybrid fuzzy-FOPID controller. The preferred velocity is set by the idle speed is 1500 RPM. The acquired findings show that the fuzzy controller produces nearly smooth thrust with minimal steady-state error. A high beginning current can be inferred from its delayed settling time and high starting torque (nearly 200% of the quoted torque). However, the FOPID driver shortens the time it takes for the system to stabilize and reduces the beginning torque (by about 135 percent of the maximum torque). However, its torque response displays noticeable waves and its steady-state error is larger than that of the fuzzy controller. Faster settling time and restricted beginning current result in less starting traction with the suggested hybrid fuzzy-FOPID controller. Although it has a slightly larger steady-state error than the fuzzy controller, the torque response exhibits much smoother operation, particularly once the motor achieves steady state. The benefits of both the fuzzy and FOPID controllers, such as quick settlement time and small steady-state error, as well as small waves and restricting the beginning current, have been combined in the created hybrid fuzzy-FOPID controller.



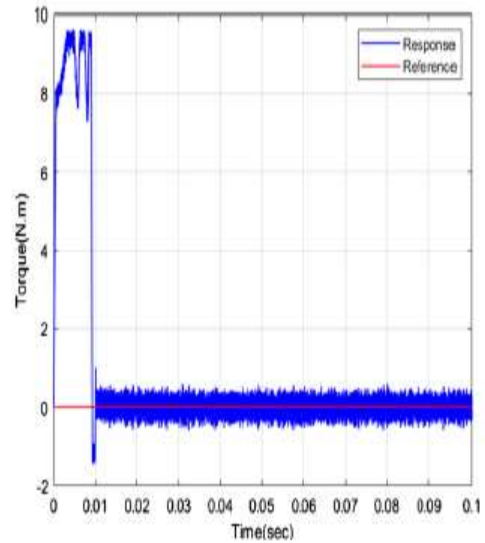
(a)



(a)



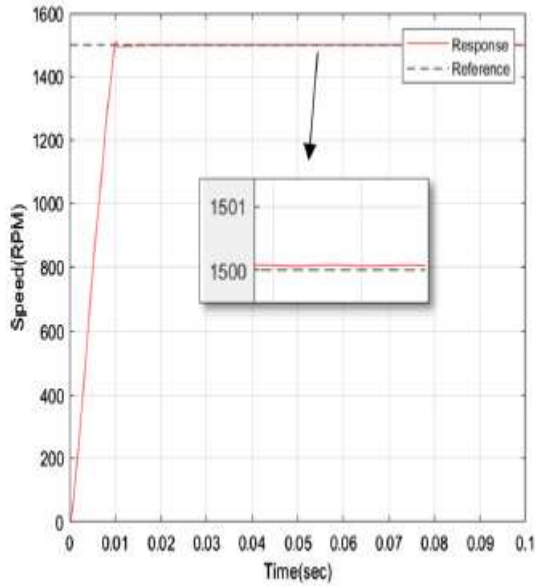
(b)



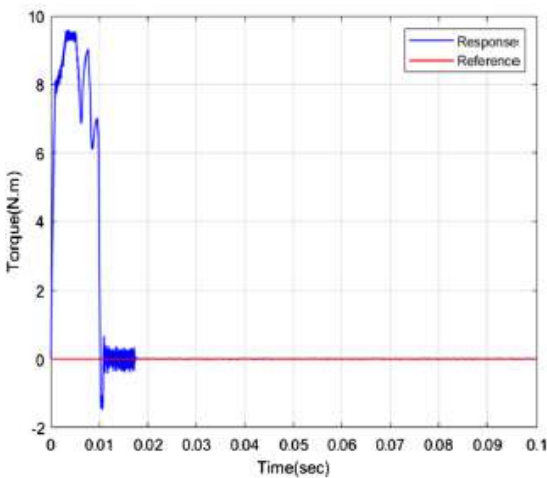
(b)

Figure 9: a) No-load speed response of a Fuzzy controller, and b) No-load torque response of a Fuzzy controller

Figure 10: a) No-load speed response of a FOPID controller, and b) No-load torque response of a FOPID controller



(a)



(b)

Figure 11a shows the no-load speed reaction of the suggested Fuzzy-FOPID regulators, b the no-load torque reaction of the suggested Fuzzy-FOPID devices

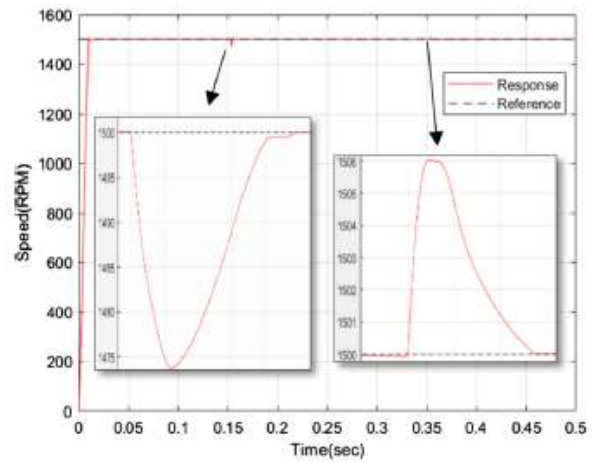
Varying Load Operation

Figures 12, 13, and 14 depict the speed and torque reactions of the motor with the fuzzy, FOPID, and the suggested fuzzy-FOPID regulators at a steady speed (1500 RPM) and varying load. Respectively. The steady-state inaccuracy and torque fluctuations of the fuzzy actuator are both modest. It can counteract the speed's fluctuation caused by changes in the burden and restore it to the predetermined level. Its instantaneous speed traits, however, show a sluggish settling time, whereas the settlement time and beginning torque of a high overrun FOPID controller

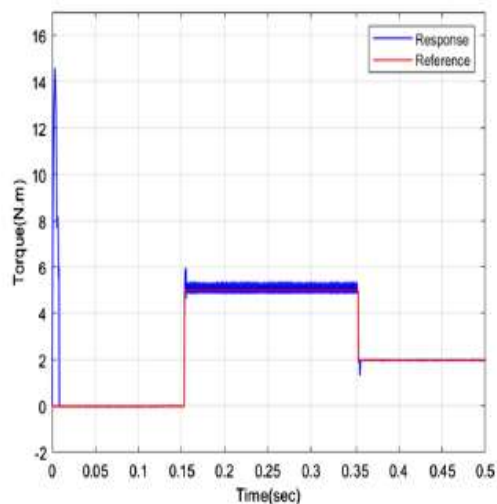
are both quick. However, it is still significantly impacted by steady-state error and high torque fluctuations, as well as changes in load. The suggested hybrid fuzzy-FOPID controller, on the other hand, offers speed response with low steady-state error and quick settling time, as well as torque response with low waves and low initial input.

Varying Speed Operation

At a fixed torque (4 N.m) and varying velocities ([300, 1500, 450]), the speed and torque reactions for fuzzy, FOPID, and the suggested fuzzy-FOPID controllers are shown. In Figures 15, 16, and 17 individually. The steady-state inaccuracy of the system based on the fuzzy controller is greatest at the lowest speed (300RPM), but it is minimal at the maximum speed. It also has the longest time to settle when speed drops from

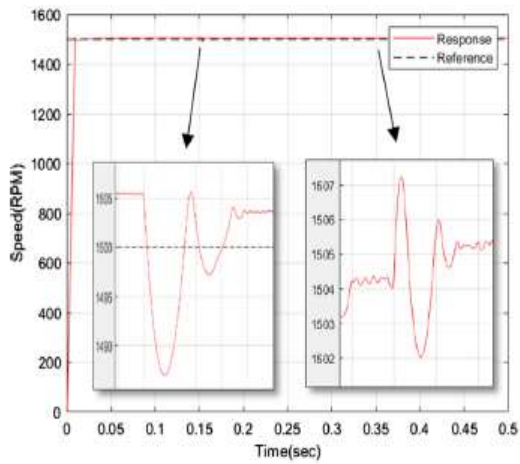


(a)

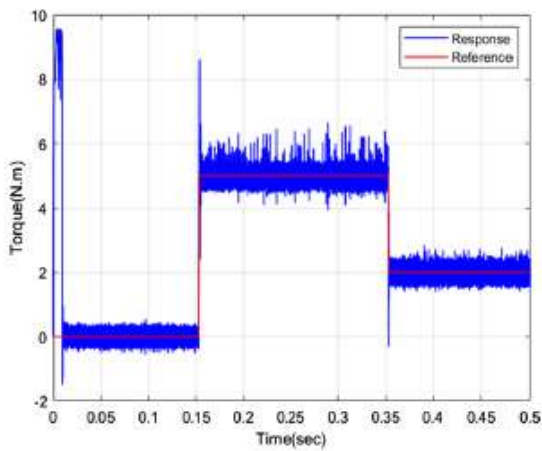


(b)

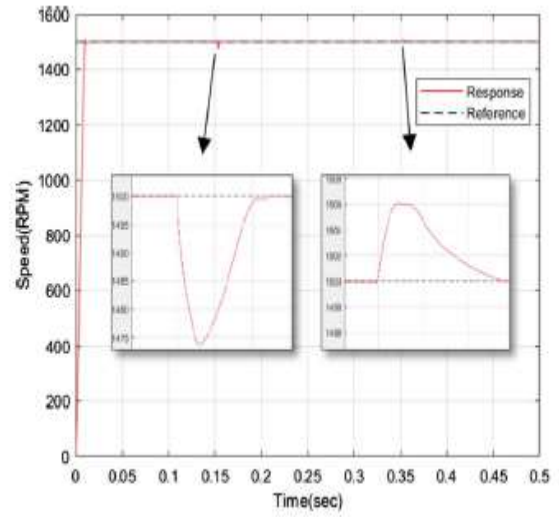
Figure 12: a Speed Response of a Fuzzy Controller with a Varying Load, and b Torque Response of a Fuzzy Controller with a Varying Load



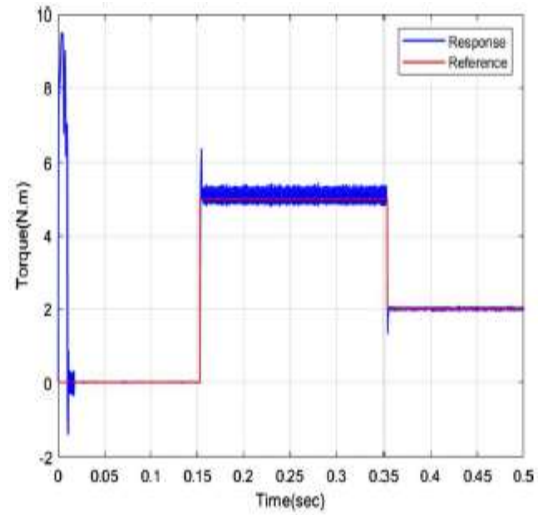
(a)



(b)



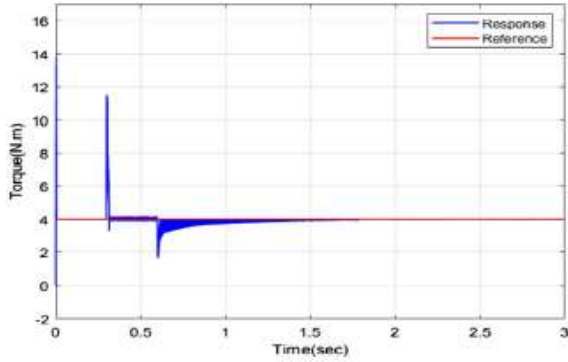
(a)



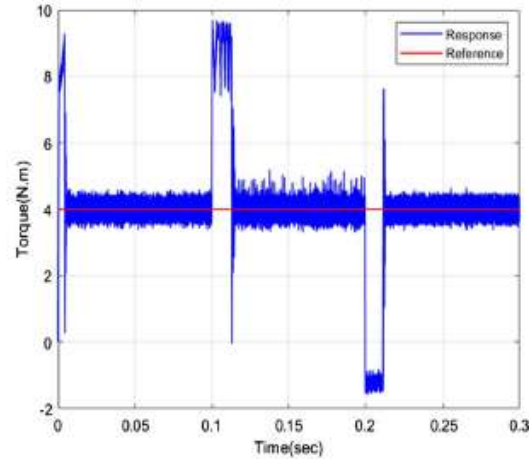
(b)

Figure 13: a FOPID controller's speed reaction to a changing load, and b its torque response to a changing load

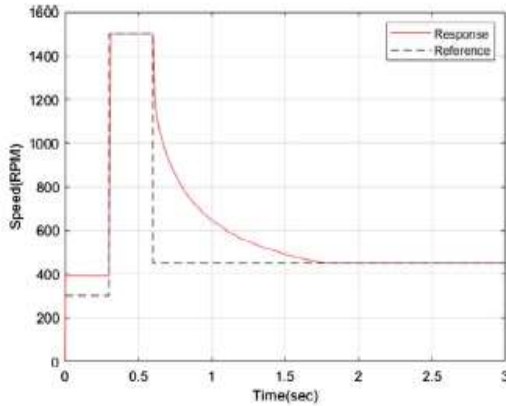
Speed (a) and torque (b) responses to varying loads for the suggested Fuzzy-FOPID controller are shown in Fig. 14.



(b)

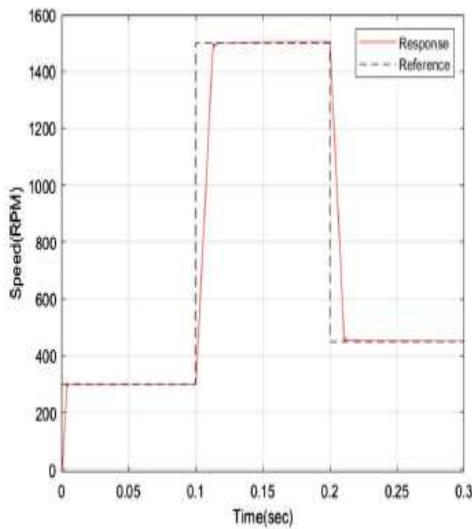


(b)



(a)

Fuzzy controller speed response at varying speeds (a) and torque response at varying speeds (b) are shown in Fig. 15.



(a)

Fig. 16 shows the speed and torque responses of a FOPID controller operating at varying speeds (a, 1500 RPM to 450 RPM, and b, 450 RPM to 1500 RPM, respectively). It has the smoothest torque reaction and the greatest resistance to torque waves. The disparity in tempo. The FOPID device has a quick reaction time and a tiny steady-state inaccuracy even at the slowest pace (300RPM). However, at other rates, the FOPID driver still exhibits the aforementioned flaws. As the pace changes, so do the power fluctuations. The suggested fuzzy-FOPID controller provides a smooth and consistent speed reaction across the board with minimal steady-state error and torque distortion. Nonetheless, the power reaction varies noticeably with the speeds.

7 Conclusions

In order to regulate the DC bus voltage of the converter and the reference current of the motor, a hybrid fuzzy-FOPID controller is suggested and developed for BLDC motors in this paper. Related to the controller's feedback current. To fine-tune the suggested hybrid fuzzy-FOPID, a customized HSA was used. The combined management strategy was compared to both the fuzzy and FOPID-based systems when used independently. The benefits of both the fuzzy controller and the rapid reaction and beginning current-limiting capacity of the FOPID controller are combined in the hybrid fuzzy-FOPID controller that is proposed. The modeling findings indicate that the motor's speed and power reactions are significantly enhanced by the hybrid fuzzy-FOPID controller.

References

1. Yedamale, P.: "Brushless DC (BLDC) motor fundamentals," Microchip Technology Inc., 2003.
2. Xia, C.L.: *Permanent Magnet Brushless DC Motor Drives and Controls*. Wiley, New York (2012)
3. Padula, F.; Visioli, A.: *Tuning rules for optimal PID and fractional- order PID controllers*. *J. Process Control* **21**(1), 69–81 (2011)
4. Cajo, R.; Mac, T.T.; Plaza, D.; Copot, C.; De Keyser, R.; Ionescu, C.: *A Survey on Fractional Order Control Techniques for Unmanned Aerial and Ground Vehicles*. *IEEE Access* **7**, 66864– 66878 (2019)
5. Chen, Y. Q.; Petráš, I.; Xue, D.: "Fractional order control – A tutorial," In: *Proceedings of American Control Conference*, pp. 1397–1411 (2009)
6. Xu, D.; Chen, Y.: *A comparative introduction of four fractional order controllers*. In: *Proceedings of the 4th World Congress on Intelligent Control and Automation*, pp. 3228–3235 (2002)
7. Termous, H.; Moreau, X.; Francis, C.; Shraim, H.: *From the standard PID to the CRONE first generation controller: Application to an anti-roll system for Electric Vehicles*. *IFAC-PapersOnLine* **51**(4), 733–738 (2018)
8. Podlubny, I.: *Fractional-order systems and fractional-order controllers*. *Inst. Exp. Phys., Slovak Acad. Sci.* **12**(3), 1–18 (1994)
9. Shah, P.; Agashe, S.: *Review of fractional PID controller*. *Mechatronics* **38**, 29–41 (2016)
10. Valério, D.; Sá Da Costa, J.: "A review of tuning methods for fractional PIDs," In: *4th IFAC Workshop on Fractional Differentiation and its Applications*, p. 13 (2010).